Measured and Predicted Response of a Submerged Towed Sonar Array to Maneuvering Input

Jaye Falls
Assistant Professor
United States Naval Academy
Annapolis, MD

Sarah E. Mouring
Professor
United States Naval Academy
Annapolis, MD

Ananth Sridharan
Research Engineer
University of Maryland
College Park, MD

Jean Loomis
Ensign
United States Navy
Annapolis, MD

ABSTRACT

There exists a necessity to increase a helicopter pilot's safety during mine countermeasure operations. Models have been developed for scenarios involving a cable that is fully submerged in either air or water, but there has been very little testing when the cable is partially submerged. This change in fluid type along the length of the cable has a significant impact on the stability and drag forces that has not yet been extensively studied. A series of experimental investigations examining speed, acceleration, length of cable and path of motion were paired with predictions from a simulation for the purpose of developing a predictive tool. These tests characterized the stability of the body, indicating that acceleration is a governing factor in the operability of the towed sonar. The simulation developed to predict the behavior of the helicopter towed submerged body predicts the fundamental behavior of the body, but does not capture hydrodynamic instabilities that result in the body leaving the water.

INTRODUCTION

There is a wide range of use for towed body systems whether it is from an aircraft or a ship. Military missions, such as mine countermeasure operations, and scientific research, such as the mapping of underwater environments, depend on the precise operation of towed bodies.

These towed sonars must be deployed from medium to heavy lift helicopters [1] due to the horsepower requirements when operating the sonar. The Navy has recently transitioned to using the MH-60 for mine countermeasure operations. The MH-60 is a smaller helicopter than the MH-53 traditionally used for towing operations, and takes up less deck space and therefore can be hosted by a greater range of ships [2].

Further, when conducting mine countermeasure operations, helicopter pilots are forced to fly low to the water and with decreased air speeds. The standard procedure for a pilot in an emergency is to increase altitude and speed, and move away from the water. When a helicopter is towing, the power margin is significantly reduced and altitude cannot be increased quickly in emergency situations. Airborne mine countermeasure operations are therefore inherently more dangerous, because there are fewer options in an emergency [4]. Because the reduced power margins during towing operation leads to a nose down attitude, the pilot's work load is increases, causing discomfort to the pilot [3].

Pilot comfort aside, there are also significant technical issues specific to a rotorcraft-towed body system. Physical properties, such as mass and inertia, are much closer for helicopters and towed bodies compared to ships and towed bodies. Helicopters also have less installed power than ships and are forced to operate with drastically smaller available margins. The partially submerged cable also has varying loading and response as the cable moves through water and air.

This rotorcraft-towed body issue has been a significant problem for the U.S. Navy and has resulted in multiple deaths. Extensive studies have been performed in modeling the aircraft-cable-towed body system, focusing on the motion of a towed object [5] and its stability [6] as it moves through air. Work also has been done on modeling a towed system underwater by Zhijiang and Liangan [7] and at the Norwegian University of Science and Technology [8]. While models have been developed for scenarios involving a cable that is fully submerged in either air or water, there has been very little research on when the cable is partially submerged, either experimentally or analytically. This change in fluid type along the length of the cable has a significant impact on the stability and drag force that has not been extensively studied.

This project is a collaborative effort between researchers at the University of Maryland and the United States Naval

Presented at the AHS 71st Annual Forum, Virginia Beach, Virginia, May 5–7, 2015.

Academy. It will focus on characterizing the stability of a towed body in an aircraft-towed body system. Lab tests also will be used to validate a tool used to predict the hydrodynamic forces acting on the towed body. The ultimate goal of this investigation is to provide guidance to helicopter pilots while conducting airborne mine countermeasure operations.

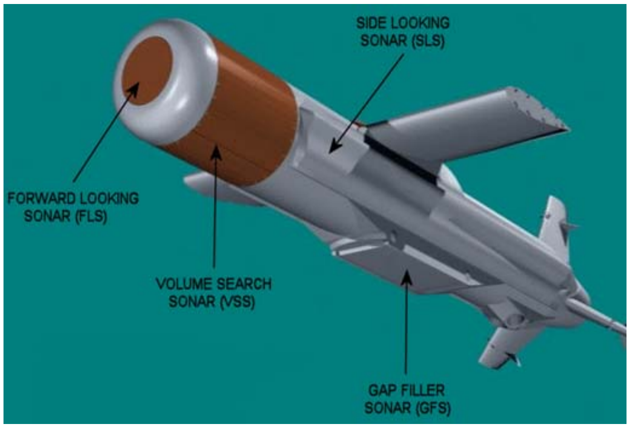

Figure 1. Raytheon AN/AQS-20A mine hunting sonar (Ref [9]).

METHODOLOGY

Model

The towed model used is a geometrically similar scale model of the Raytheon AN-AQS-20A mine hunting sonar (see Figure 1).

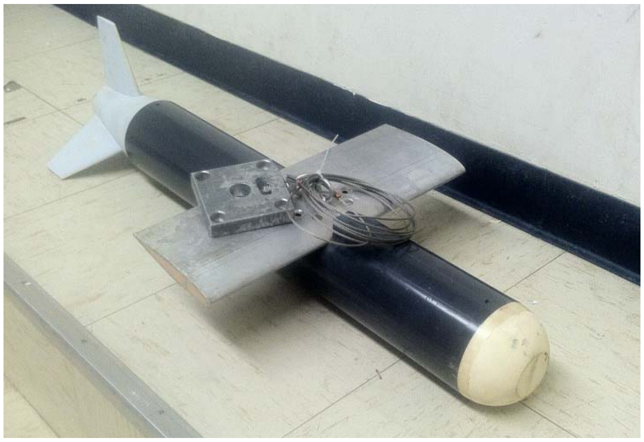

Figure 2. Picture of testing model the 3.4m cable and plate used to attach to the force gages.

The model shown in Figure 2 is a passive towed body with fixed pitch wings. The wing is mounted with a 5° nose down tilt to maintain the down force on the body at it moves through the water. The three tail fins are mounted 120° apart. The model is simplified from the sonar seen in Figure 1 and does not have any of the bottom mounted features. The model is constructed of PVC schedule 80 pipe, the wing is a NACA 0015 aluminum extrusion, and the nose and tail are a plastic composite produced by rapid prototyping [10]. The body is hollow inside with an adjustable weight system that can be used to manipulate the center of gravity of the body forward and aft. For these tests, the center of gravity was adjusted so that it was immediately below the tow point. The geometry of the model is fully described in Table 1.

Table 1. Principal Characteristics of Towed Body Model.

Characteristic	Value
Nose to Leading Edge of Wing	0.914 m
Nose to Tow Point	1.016 m
Nose to Leading Edge of Tail Piece	2.032 m
Nose to End of Body	2.235 m
Diameter of Body	0.250 m
Length from Wingtip to Outer Edge of Body	0.400 m
Width of Wing	0.200 m
Width of Body	0.250 m
Height of Body	0.610 m
Wingtip to Wingtip Width	1.050 m
Scale factor (full:model)	3.7

Cable

The cable chosen for this test was a 0.254 cm diameter, 7 x 19 stainless steel wire. The diameter was chosen for a Strouhal number that would not produce strumming at the range of test speeds selected. This concern is only relevant in lab testing because fairings are attached to the cable at full scale operations to prevent any vibrations [11], [12].

Varying the cable length will impact the periodicity of the body's movement, similar to a simple pendulum (Equation 1), where L is the length of the cable, g is gravity, and T is the period of the pendulum.

$$T = 2\pi \sqrt{\frac{L}{g}} \tag{1}$$

In full scale rotorcraft-towed body systems, a normal cable length is around 200 m. Even scaled to fit the model, that would require over 50 m of cable, which is more than half of the total tow tank length. Therefore, the tow tests were conducted with cable lengths of 1.7 m, 3.4 m, and 4.6 m. The longest cable length keeps the towed body from hitting the tank walls or bottom during any testing. By varying the cable length, the impact of effective length can be assessed and extrapolated for operational use.

A double pendulum is a more complex model in which one pendulum is attached to the bottom of another pendulum. This model was examined as a possible physical analog to the cable-towed body system, where the dry section of the cable represents the upper pendulum and the wet section of the cable (with the attached body) is the lower pendulum [13]. Using this model, it was predicted that small amplitude motion of the dry part of the cable, represented by the dashed line in Figure 3, would result in similar motions of the towed body but with much larger amplitudes.

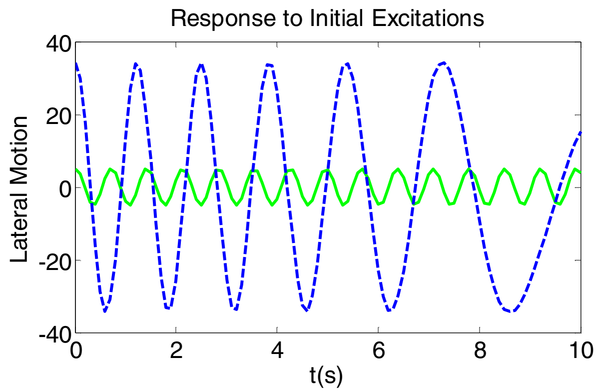

Figure 3. Predicted normalized motion of the towed body, modeled as a double pendulum in one fluid. The solid line represents the motion of the cable at the free surface of the water and the dashed line represents the motion of the towed body.

Simulation Methodology

The simulation was developed by Dr. Ananth Sridharan at the University of Maryland to predict the forces acting on a rotorcraft-towed body system [14]. The model uses most of the physical characteristics of the cable-towed body system: the physical properties of the towed body and of the cable, and the interaction between the cable and the water including of the tow point with respect to the free surface. Predicted values include: the body's velocity, the associated cable force, the body's location with respect to the tow point, the cable's angle to the horizontal, and the cable's angle at each quadrature.

The program models the position of the towed body by using Euler-Bernoulli beam theory to determine the deflection of the cable. Essentially, the end of each segment acts as a pivot point around which the following segment moves. These various segments are combined through a cascade of rotation matrices in order to convert the deflection into an earth-fixed system [15]. This multi-body approach ensures that the forces acting on the cable are modeled accurately when the beam is segmented into multiple different pieces.

The simulation also employs an intermediate cable fixed system to translate the model into the more easily understood earth-fixed system. The rotation matrix converts the vector components from the root of the first segment, the hook, to the root of the second segment, and the second segment to the root of the third and so on. These matrices take into account the elastic displacement of each individual beam segment of the cable.

As the cable and body are towed through the water, buoyancy, drag, and gravity will act on the cable. The tangential drag on the cable is due to viscous forces. This drag force is characterized using experimental data from Knutson, which indicates that the force per unit diameter will remain constant with a coefficient of 0.0249. Viscous forces in combination with pressure differences account for the normal drag. Knutson's experimental data was used to determine that the drag coefficient can vary from 0 to 1.7 [16]. The coefficient is determined by the nature of the elastic axis and where it lies relative to the flow orientation.

The simulation uses the critical geometry of the towed body to relate the motion of the cable to the tow point and then to the center of gravity of the towed body. It employs the same transformation matrixes used with the cable to relate the location of the tow point to the speed and acceleration of the rest of the body. The external forces acting on the body are calculated using the same method as the cable.

Testing Methods

All experimental testing was conducted in the 115.8 m tow tank in the Hydromechanics Laboratory at the United States Naval Academy. Three different types of tests were conducted in an effort to characterize the hydrodynamic forces acting on the cable-towed body system.

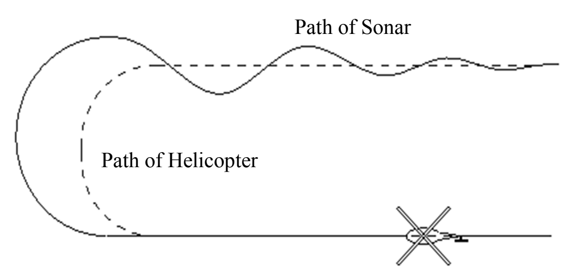

Figure 4. The maneuver the testing will be simulating.

The testing matrix was designed to capture the behavior of the body after it has been towed through a change of direction, as shown in Figure 4. The first phase of testing was used to develop a fundamental understanding of the body's stability while it was undergoing motion in a straight line while also studying the impact on lift and drag. The test matrix methodology was based off of the desire to find an operating envelope for various velocities and accelerations (Figure 5 (a)).

The Planetary Motion Mechanism (PMM) is mounted on a tow carriage, and is capable of producing oscillatory motion of the tow point at a range of amplitudes and frequencies. In the second phase, after the body reaches equilibrium position behind the tow point, the PMM was displaced so that the tow point was 0.6096 m to starboard. The body's reaction to the rapid impulse was then observed at different speeds and cable lengths. A schematic of the predicted motion of the body and PMM can be seen below in Figure 5 (b).

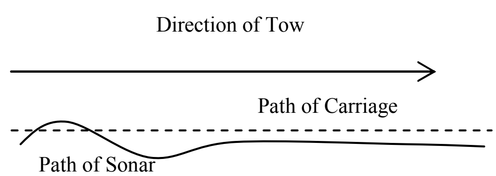

5(a): First Testing Method

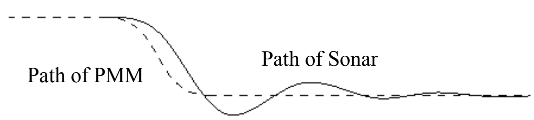

5(b): Second Testing Method

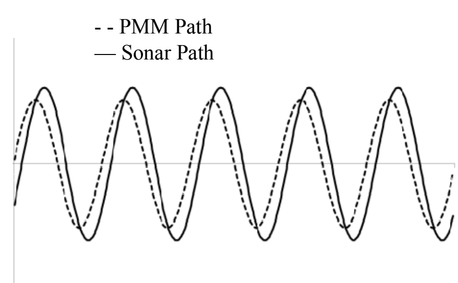

5 (c): Third Testing Method

Figure 5: Table describing the tow testing methods and the anticipated sonar body response.

The third testing method used full harmonic motion of the tow point to record the body's ability to follow the hook at different frequencies and cable lengths. The anticipated motion is shown in Figure 5 (c). The goal is to examine the the lag time between the movement of the hook and the response of the body, and determine how the lag time varies with the frequency of the hook motion.

RESULTS AND DISCUSSION

Straight Line Testing

As the body was tested under different speeds and accelerations, it was observed that step increases in velocity led to stable body position compared to a continuous increase in velocity. Furthermore, as long as the initial position of the body was aligned with the direction of motion, the stability was maintained for the range of speeds tested. Any other initial position produced kiting and oscillations for some period of the tow. To better approximate the transient behavior of the towed body during turning maneuvers, the initial position was backwards to the motion of tow.

The relationship between lift and drag also informed the angle between the towed body and the cable, where the angle is defined as the distance between the body and the cable (Figure 6). The angle between the body and the cable decreases as the speed increases, and the body is therefore located further behind the carriage as the speed is increased.

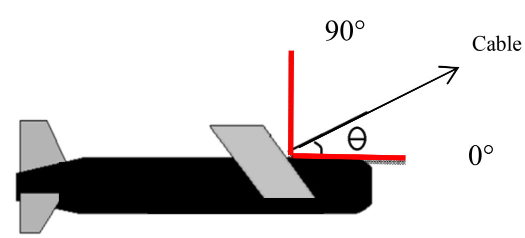

Figure 6. Sonar with cable attached.

Speed (m/s)	Accel. (m/s^2)	Avg. Lift (N)	Avg. Drag (N)	Stability Condition
0.61	0.31	6.57	0.85	Submerged
1.83	0.61	10.03	6.33	Submerged
1.83	0.76	11.01	8.80	Surfacing
1.83	0.91	10.63	8.35	Surfacing
2.44	0.46	13.24	9.22	Surfacing
2.44	0.61	12.32	8.77	Surfacing
2.44	0.76	10.12	9.29	Surfing
2.44	0.91	8.85	8.12	Surfing
3.05	0.61	12.38	12.13	Surfing
3.05	0.76	8.92	10.13	Surfing
3.05	0.91	11.82	11.68	Surfing
3.05	1.07	8.30	10.63	Surfing
3.66	0.31	7.80	11.97	Surfacing
3.66	0.61	0.12	8.04	Surfing

Table 2. Test matrix and result of straight line testing

From these initial observations, three states were developed to describe the motion of the body: submerged, surfacing, and surfing. The submerged state describes when the body stayed submerged for the whole run. There may have been slight kiting at the beginning and end of each run, but there were never any drastic spikes in either lift or drag force. During the "submerged" state, a rotorcraft pilot would not experience difficulty maneuvering the aircraft and the sonar would be able to collect data for the whole run.

The surfacing state describes when the body kites dramatically and momentarily leaves the water, but eventually reenters the water and returns to the centerline position behind the carriage. There are spikes in both lift and drag in the surfacing state that would be difficult for the pilot to handle; however, these spikes tend to occur in the same place: between the start of movement and when the body exits the water. When the body reenters, there is a smaller increase in forces (see Figure 7). This state is not ideal because if the body leaves the water in real conditions, it is exposed to the sea state and wind and the sensors are not collecting data.

The surfing state is when the body kites to the side and leaves the water so violently that it inverts and then is dragged along the surface. There also are spikes in lift and drag force that accompany this state and would increase the pilot workload. Again, in real operations this would expose the sonar body to the sea state and wind as it is dragged along the surface of the water, and the sensors could not be used.

These three conditions were used to establish an operating envelope to determine at what speeds and accelerations the sonar will remain useful for data collection (Figure 8).

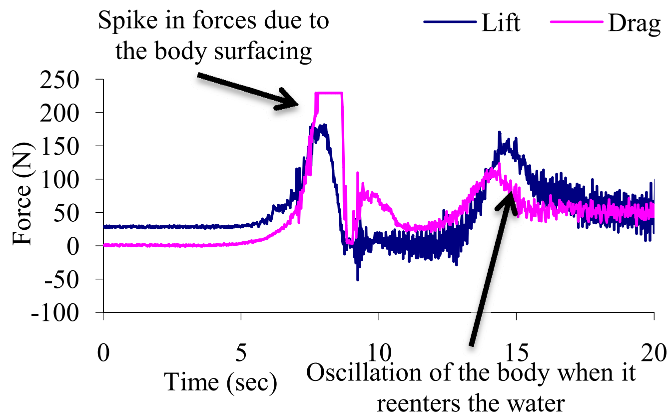

Figure 7. Time history of the lift and drag forces of the body at 3.048 m/s, accelerating at a rate of 0.6096 m/s^2.

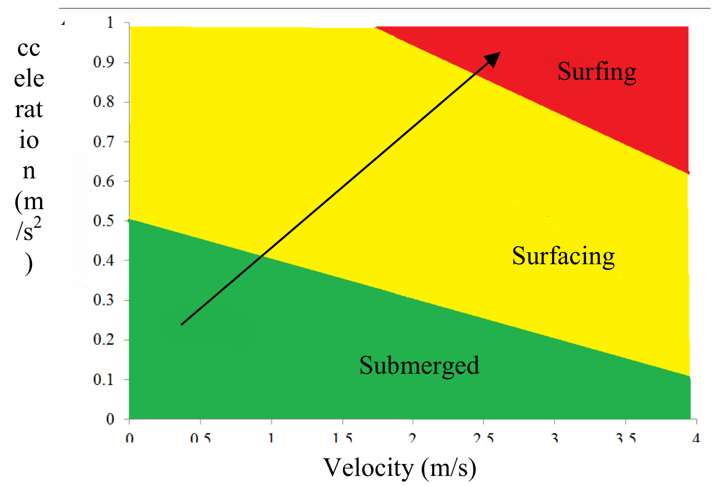

Figure 8. Graph describing the operability of the model scaled sonar with respect to acceleration and velocity.

Ideally, the pilot would always maintain lower speeds and accelerations; however, there is a sizeable buffer area of speeds and accelerations where the sonar will remain stable and be effective. The only caveat to these middle velocities and accelerations is that the pilot might have to cope with a spike in the lift and drag force due to initial instability of the towed body position. Also, the pilot will have to take into consideration the effect of sea state and wind on the body if it leaves the water. Mine countermeasure operations will not likely be conducted in sea states greater than one or two or when the wind is very strong; however, any type of wave or wind force will need to be taken into account if the pilot chooses to accelerate to a velocity in the yellow surfacing zone because the body could, at some point, experience wind and wave forces. This environmental exposure is particularly a risk with shorter cable lengths.

Impulse Testing

For operational efficiency, the pilot wants the body to find the equilibrium tow position quickly so that he can maximize time within the search grid, commonly known as "staying in the lane". As such, the damping coefficient of the sway force plotted against time would be the best measure of how quickly the body stops oscillating and moves in a straight line. Table 3 shows the complete matrix of speeds and cable lengths tested.

Table 3. Test matrix and results of the damping coefficients at varying speeds and cable lengths

Damping Coefficients (s^{-1})	**Cable Lengths (m)**		
Velocity (m/s)	**1.7**	**3.4**	**4.6**
1.22	-	0.268	0.179
1.83	0.295	0.156	-
2.44	0.235	-	-
3.05	-	-	-

Figure 9 shows an example of the motion of the body and the damping coefficient. The red vertical line indicates when the PMM is displaced and the blue line indicates when the carriage began to decelerate. The blue dashed line represents the movement of the tow point, while the black curved line is the towed body's path relative to the tow point. Finally, the green dotted line represents the exponential decrease of the towed body's motion. For this particular run the damping coefficient was 0.268 s^{-1}.

The damping coefficient (λ) was determined using a logarithmic decrement method (Equation 2).

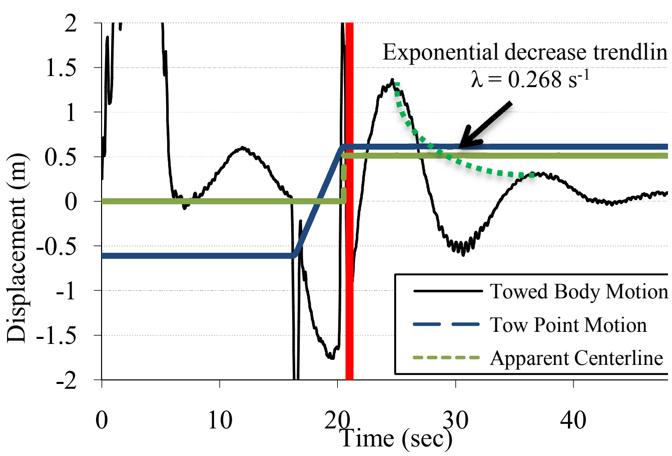

Figure 9. Representative time history of impulse testing.

The *max* is the first local maximum of the body's path of motion and the *min* is the second local maximum. The damping coefficient has a unit of s^{-1}.

$$\lambda = \frac{1}{2\pi} \ln\left(\frac{max}{min}\right) \tag{2}$$

As such, the towed body had to complete two full oscillations to determine the damping coefficient. The length of the tow tank prohibited the towed body from completing two full oscillations for higher speeds and for the 4.6 m cable. These testing limitations are reflected in the incomplete results in Table 3.

As speed increases, the damping coefficient decreases and as the cable length increases, the damping coefficient also decreases. As such, the 1.7 m cable at 1.8 m/s had the greatest damping coefficient at 0.295s^{-1}. This cable length and speed cause the towed body to return to centerline the most efficiently of all of the speeds and cable lengths tested (Figure 10).

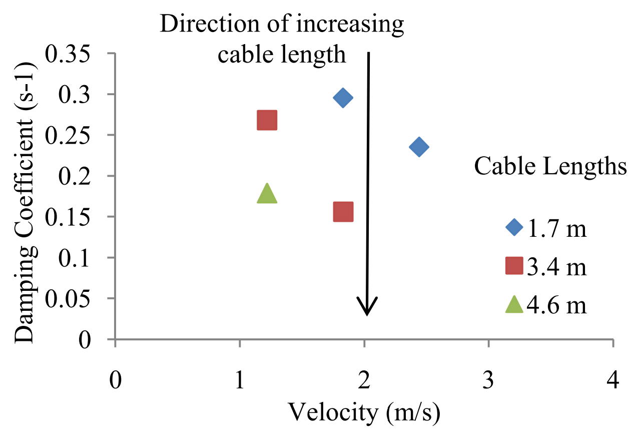

Figure 10. The relationship between the damping coefficient and velocity for the three cable lengths tested.

Full Harmonic Motion Testing

The goal of this test is to examine the response of the towed body to varying oscillation frequencies of the PMM. Oscillating the tow point as a frequency of 0.025 Hz resulted in very long lag times of 10-16 s. On the other hand, 0.125 Hz was too fast and did not allow the body to complete a full oscillation before being pulled back. For the 1.7m and 3.4 m cable lengths, full harmonic motion did not occur; thus, the data given for the frequency of 0.125 Hz in these two cases.

Figure 11 is a representative run from the full harmonic motion tests, and shows towed body displacement versus time. The red vertical line represents the start of the carriage's forward motion and the blue vertical line represents when the carriage stops at the end of the tank.

The lag time of the body decreases with increased frequency of the towing input while increasing with cable length (Figure 12). Across the range of frequency from 0.025 to 0.075 Hz, the two shorter cable lengths show a similar trend in body response time. However, the 4.6 m cable length is more sensitive to the frequency of the towing input, and the rate of the lag time is significantly different. As the frequency of the towing input increases, the towed body with 4.6m cable length shows rapidly decreasing lag times.

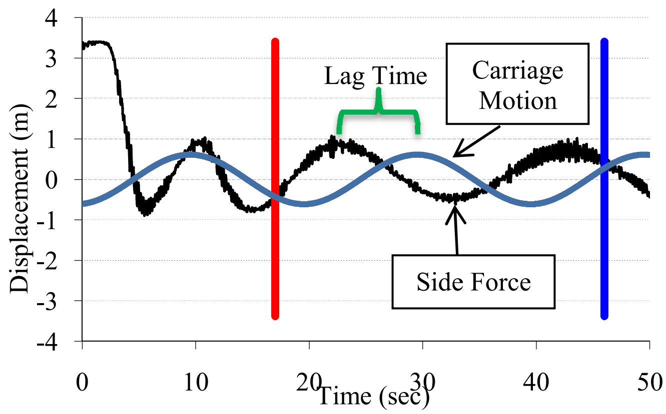

Figure 11. A representative time history of full harmonic motion conducted during the second phase of testing. (Frequency = 0.05 Hz, 3.4 m tow cable.

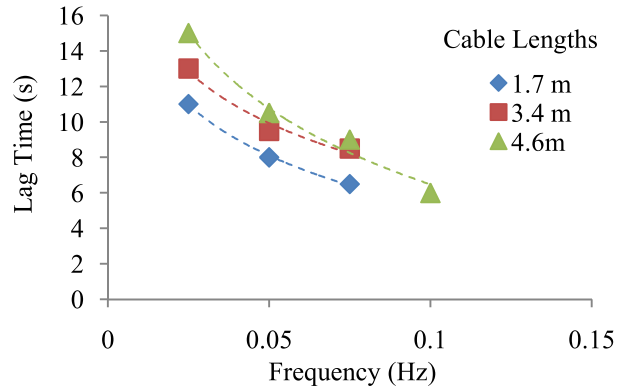

Figure 12. A summary of the lag time of the towed body at varying frequencies and cable lengths.

Simulation

For this part of the investigation, the simulation has been used to investigate straight-line towing, which corresponds to the first phase of experimental testing. First, the movement and position of the towed body was analyzed. Figure 13 shows the towed body depth and cable angle at a speed of 2.4 m/s and an acceleration of 0.6 m/s^2. As discussed above, this was found to be a surfacing condition in the experiments. The prediction does not capture the body surfacing behavior, and instead shows a relatively constant body depth for the length of the tow. The cable angle shown is the variation from vertical: 0 degrees means that the cable is hanging straight down, 90 degrees means that the cable is horizontal behind the towing hook. As seen in Figure 13, as the body velocity increases from a standstill to 2.4 m/s, the cable gradually extends behind the towing hook, and reaches a mean position. There is some oscillation about the mean that is larger than any observed in testing.

A comparison of measured and predicted cable angles further demonstrates that the prediction is capturing the trend of the experimental results, but not operational instabilities such as surfacing or surfing, which tend to occur at higher tow accelerations. The following figures show results for one cable length, 3.4m, and two accelerations, 0.3 m/s^2 and 0.6 m/s^2. In Figure 14, the predicted force in the cable is higher than measured, but shows the correct trend from 2.4 m/s to 3.0 m/s. At 3.6 m/s, the measured results show significant decrease in force as the body surfaces and kites, particularly at the higher acceleration. In contrast, the prediction indicates a steady increase in force as if the body remains beneath the water surface at all accelerations. The predicted cable force is also relatively insensitive to tow acceleration, and at each velocity shown, the two accelerations examined show nearly the same cable force.

Figure 15 shows a similar comparison for cable angle. In this case, the predicted angles are significantly smaller than the measured angles, but the trends show good agreement across the range of velocity. The two measured angles that are significantly different from prediction correspond to high acceleration, surfacing or surfing conditions.

These initial results from the simulation indicate that the fundamental behavior of the towed body in straight line motion has been appropriately modeled. However, extreme conditions where the body broaches the water surface are not within the scope of the current modeling. The best results occur at low acceleration conditions, where the trends are captured but the magnitudes of force and cable angle are not accurate.

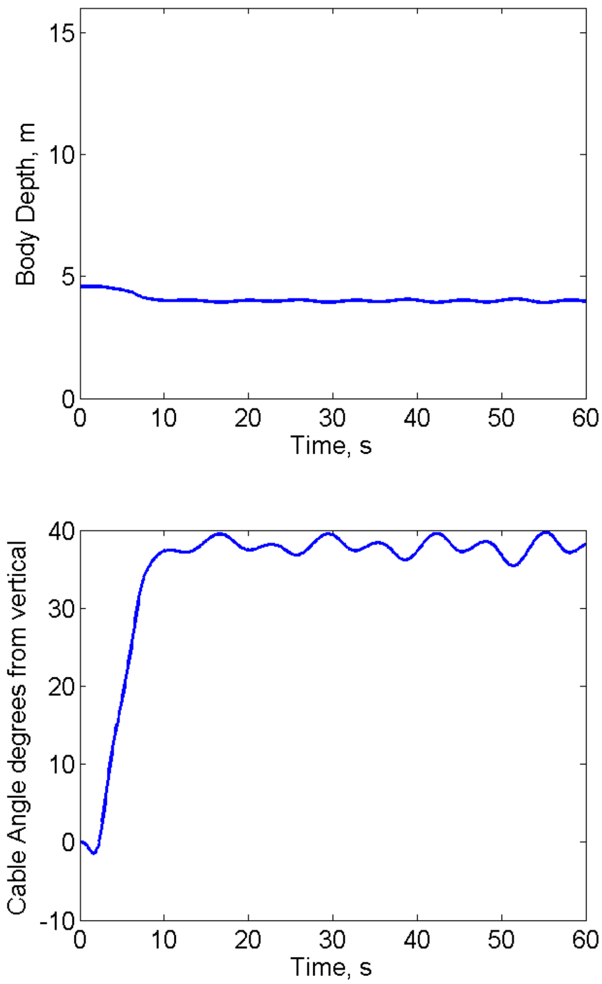

Figure 13. Prediction of towed body depth and cable angle at 2.4 m/s, 0.6 m/s^2, and cable length = 3.4m.

CONCLUSIONS

1. Experiments have shown that gradual step increases in velocity (velocity stepping) from rest increase operability of the sonar and reduce hydrodynamic forces, compared to continuous velocity increases (velocity ramping). When velocity ramping is necessary, keeping acceleration low can improve positional stability by reducing surfacing and surfing.

2. When the body faces the direction of intended motion, the body remains stable and the hydrodynamic forces are decreased. Some amount of positional instability can be expected when the direction of motion and the initial body position vary.

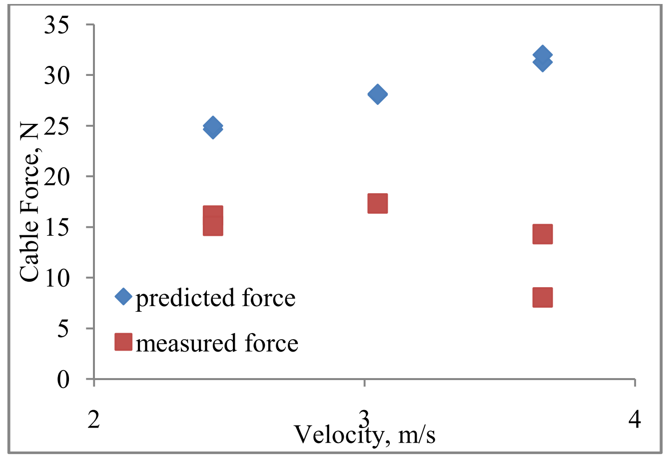

Figure 14. Comparison of measured and predicted cable force for two tow accelerations, 0.3 m/s^2 and 0.6m/s^2.

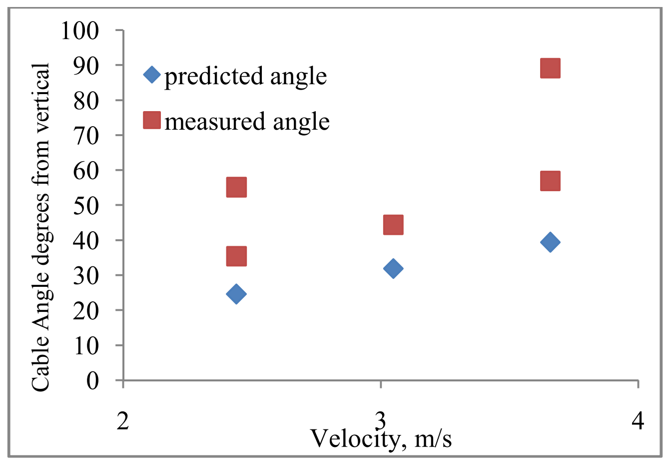

Figure 15. Comparison of measured and predicted cable angle for two tow accelerations, 0.3 m/s^2 and 0.6m/s^2.

3.

4.

5. The damping coefficient decreased with an increase in speed and cable length. This results in more body oscillation and longer times required for the body to find equilibrium position.

6. Lag time increased with an increase in cable length, but decreased with an increase in oscillating frequency of PMM.

7. The current iteration of the simulation accurately predicts the depth position, and captures trends for cable

forces and angles for conditions where the towed body remains submerged. However, correlation is moderate to poor for conditions such as high acceleration, when the body broaches the water surface.

ACKNOWLEDGMENTS

This work is supported by the U.S. Army/ U.S. Navy/ NASA Vertical Lift Research Center of Excellence grant number W911W6-11-2-0012. The author would like to thank John Zseleczky, Dan Rhodes, and Bill Beaver at the Hydrodynamics Laboratory at the United States Naval Academy for all of their expertise. Linda Adlum's support also was critical in compiling the simulation. Finally, LCDR Ethan Lust, USN, brought this project into the realm of reality with his flight experience.

REFERENCES

[1] Department of the Navy, "Naval Air Training and Operating Procedures Standardization," 2005.

[2] "LCS & MH-60S Mine Counter-Measures Continue Development," *Defense Industry Daily,* 16 November 2014.

[3] L. U. Ethan Lust, Interviewee, *Personal communication.* [Interview]. 9 February 2015.

[4] D. A. Chapman, "Effects of ship motion on a neutrally-stable towed fish," *Ocean Engineering,* vol. 9, no. 3, pp. 189-220, 1982.

[5] N. Nakagawa and A. Obata, "Longitudinal stability analysis of aerial-towed systems," *Journal of Aircraft,* vol. 29, no. 6, pp. 978-985, 1992.

[6] B. Etkin, ""Stability of a Towed Body"," *Journal of Aircraft,* vol. 35, no. 2, pp. 197-205, 1998.

[7] Y. Zhijian and J. Liangan, ""A dynamic model to maintain the depth of underwater towed system"," in *2012 International Conference on System Science and Engineering*, Dalian, China, 2012.

[8] J.Leria and T. Jacobsen, ""Numerical and Experimental Studies of Submerged Towing of a Subsea Template"," NTNU, 2012.

[9] Raytheon, "AN/AQS-20A Minehunting Sonar System," Tewskbury, Massachussets, 2008.

[10] J. Falls, ""Hydrodynamic Characterization of a Sonar Body for Rotorcraft-based Towing"," American Helicopter Society Internationl, Quebec, 2014.

[11] B. Munson, D. Young, T. Okiishi and W. Huebrech, Fundamentals of Fluid Mechanics, 2009.

[12] B. Sunden, "Vortex Shredding," *Thermopedia,* 2011.

[13] L. Meirovitch, Fundamentals of Vibration, McGraw-Hill, 2011.

[14] A. Sridharan and R. Celi, "On the Role of Cable Curvature in Rotorcraft-based Tow Operations for Submerged Loads," in *American Helicopter Society*, Quebec, 2014.

[15] A. Sridharan, Tow Tank Simulation Program, College Park: University of Maryland, 2013.

[16] R. Knutson and R. Singleton, "Operation and Hydrodynamic Evaluations of a Controlled-Depth Towed Depressor Designed to House a Conductivity, Temperature, Depth (CTD) Instrument System," DAVID W TAYLOR NAVAL SHIP RESEARCH AND DEVELOPMENT CENTER , Bethesda, MD, 1981.

[17] Department of the Navy, Naval Air Training and Operating Procedures Standardization, Washington, D.C.: Department of the Navy, 2005.

[18] R. Celi, J. Falls and A. Sridharan, ""Flight Dynamics and Control of Rotorcraft Towing Submerged Bodies"," VLRCOE Year End Review, College Park, 2013.